

## ARTICLE OPEN



# Complex effects of chytrid parasites on the growth of the cyanobacterium *Planktothrix rubescens* across interacting temperature and light gradients

Joren Wierenga<sup>1</sup>, Mridul K. Thomas<sup>1</sup>✉, Ravi Ranjan<sup>2,3</sup> and Bas W. Ibelings<sup>1</sup>

© The Author(s) 2022

Chytrids are important drivers of aquatic ecosystems as phytoplankton parasites. The interaction between these parasites and their hosts are shaped by abiotic factors such as temperature and light. Here, we performed a full-factorial experiment to study how temperature and light interact to affect the dynamics of the bloom-forming toxic cyanobacterium *Planktothrix rubescens* and its chytrid parasite. We used a dynamic host-parasite model to explore how temperature and light affect long term dynamics. At low temperatures, chytrids do not survive. Higher light and temperature levels stimulated both phytoplankton and chytrid growth, with complex effects on their dynamics. Model exploration indicates that increasing temperature and light shifts equilibrium outcomes from *P. rubescens* persisting alone to stable coexistence and then to limit cycles. This provides an alternative biological explanation for why *P. rubescens* is mainly found in the relatively cold and dark lake metalimnion – it may enable avoidance of its parasite. Our study emphasizes the importance of investigating how abiotic factors interact with biotic interactions to drive complex outcomes.

ISME Communications; <https://doi.org/10.1038/s43705-022-00178-5>

## INTRODUCTION

Cyanobacteria are important primary producers in aquatic systems [1] that can be harmful when they form dense blooms, which sometimes contain high toxin concentrations [2–4]. *Planktothrix rubescens* is a common cyanobacterium that often produces toxic blooms, with high concentrations of hepatotoxins like microcystins or neurotoxins like anatoxin-a [5, 6]. It is typically found in the metalimnion of deep stratifying lakes, and performs better at lower light and temperature levels than other cyanobacteria [7–11]. It has an efficient light-harvesting complex composed of phycocyanin and phycoerythrin in addition to chlorophyll, which allows it to photosynthesize at these low light levels [12, 13]. But even though *P. rubescens* is able to grow at low light and temperature, its growth rate increases with temperature and light, and is highest at values well outside the range it typically experiences in its natural habitat. Why *P. rubescens* is rarely seen in high-light, high-temperature conditions that would appear to favour its growth remains an open question. One possible explanation that we investigate here is that temperature and light shape biotic interactions such as parasitism.

Phytoplankton growth rates increase with light and temperature up to optimal values [14], and decrease thereafter – slowly for light, very rapidly for temperature i.e. they are oppositely skewed unimodal functions [15–17]. The optimal temperature and light conditions for *P. rubescens* are poorly constrained based on existing experiments, but Oberhaus et al. (2007) measured growth rates at 15 & 25 °C and showed that it was faster at 25 °C. This implies an

optimum temperature close to or above 25 °C because growth rate decreases rapidly above the optimum temperature [17]. Similarly, Bright & Walsby (2000) and Oberhaus et al. (2007) found no meaningful decrease in growth till the maximum irradiance levels they measured in white light (200 and 300  $\mu\text{E m}^{-2} \text{s}^{-1}$ ) [13, 18]. The optimum may be lower than this at 10–15 °C, but the measured difference in growth rate was well within the range of experimental error and an optimum above 200  $\mu\text{E m}^{-2} \text{s}^{-1}$  cannot be ruled out at these temperatures either. But in lakes, the species appears to be most abundant at temperatures of 10–15 °C, although this is based on limited data; abundance peaks at temperatures from 6.5 to 20 °C have been seen [7, 19–22]. And it is often found at the depth where irradiance is 0.1–1% of that at the surface ( $\sim 1\text{--}20 \mu\text{E m}^{-2} \text{s}^{-1}$ ). They maintain themselves at this depth through light-mediated buoyancy regulation, with lift provided by gas vesicles and offset by carbohydrate ballast [23].

The dynamics of cyanobacteria are driven not just by abiotic factors such as temperature and light, but also by biotic interactions with predators and parasites [24–26]. Parasites are important but neglected biotic drivers of ecological dynamics, commonly affecting cyanobacteria as well as other species of phytoplankton [27–30]. Parasites have been shown to impact host populations of primary producers, with knock-on effects at higher trophic levels and on community structure [31–35]. One of the most ubiquitous groups of aquatic parasites is the Chytridiomycota, a large and diverse group of fungi that are best known for the role they are playing in amphibian extinctions worldwide

<sup>1</sup>Department F.A. Forel for Environmental and Aquatic Sciences and Institute for Environmental Sciences, University of Geneva, Geneva, Switzerland. <sup>2</sup>Helmholtz Institute of Functional Marine Biodiversity at the University of Oldenburg (HIFMB), Ammerländer Heerstraße 231, D-26129 Oldenburg, Germany. <sup>3</sup>Alfred-Wegener-Institute, Helmholtz-Centre for Polar and Marine Research (AWI), Am Handelshafen 12, 27570 Bremerhaven, Germany. ✉email: mridul.thomas@unige.ch

Received: 2 March 2022 Revised: 22 August 2022 Accepted: 13 September 2022

Published online: 30 September 2022

[36–38]. Chytrids have complex life cycles (described in [39]) and also infect many species of algae and cyanobacteria, including *P. rubescens*. They are often involved in the termination of blooms of cyanobacteria and other phytoplankton [40–44]. Chytrids can act as a shunt in aquatic ecosystems, transferring nutrients and carbon to higher trophic levels through infection of phytoplankton that are otherwise resistant to grazing [45–47].

The chytrid parasite is also affected by temperature and light, not just through the direct effects of temperature on its physiological processes, but also through temperature and light effects on the host [9–11, 48, 49]. For example, light affects the release of dissolved organic carbon (DOC) by phytoplankton [50, 51], which subsequently impacts chemotaxis of chytrid zoospores, and thus infection dynamics [9, 11, 52, 53]. However, we know little about how light and temperature interact to affect chytrid infections generally, and even less in the case of *P. rubescens*. Much of the work on chytrid-host interactions has been done on the diatom *Asterionella formosa* and its associated chytrids, *Rhizophydium planktonicum* and *Zygorhizidium planktonicum*. In these host-parasite pairs, both low temperature and low light can (independently) provide refuge for the host [9, 52]; ‘refuge’ in this case indicates a set of environmental conditions that prevents chytrid infection and not a physical location. *Asterionella* appears to have both a low-temperature and a high-temperature refuge, indicating that the physiological tolerance range of chytrids is narrow relative to at least some phytoplankton [48]. For *P. rubescens*, only low temperatures have been shown to offer a refuge from chytrid infections with high temperatures not investigated [10]. The closely-related species *Planktothrix agardhii* does appear to have a high-temperature refuge; McKindles et al. (2021a) found that chytrid infection rates (measured as % increase in filaments infected per day) declined above approximately 22 °C to nearly zero by 29 °C [49]. This environmental sensitivity of the chytrids has important consequences for *P. rubescens*, which is believed to experience substantial variation in temperature and light due to its typical habitat in the metalimnion. Understanding how the environment shapes the dynamics and location of *P. rubescens* requires us to examine how these abiotic factors interact to shape its growth and biotic interactions. The size and complexity of the necessary experiments means that they are rarely performed, weakening our ability to understand how environmental change affects natural populations and communities.

Here we investigated how light and temperature interact to shape *Planktothrix*-chytrid interactions using a combination of experiments and theory. We performed a full-factorial experiment that features four temperatures, four light levels and two infection status levels (infected and uninfected *P. rubescens* cultures). We extended a dynamic host-parasite model [54–57] to explore the consequences of temperature-light interactions for *P. rubescens*-chytrid dynamics. To examine this specific system, we made model parameters dependent on temperature and light and estimated them from our experiment where possible. We then investigated whether the thermal refugium for *P. rubescens* depends on light intensity, indicating that abiotic interactions shape these ecologically important biotic interactions. We demonstrate that increasing light and temperature stimulated both phytoplankton and chytrid growth, with complex effects on host-parasite interactions.

## MATERIALS AND METHODS

### Experimental design

We used a full factorial experimental design with 4 temperatures (6, 11, 16, and 21 °C), 4 light levels (2, 7, 14 and 21  $\mu\text{E m}^{-2} \text{s}^{-1}$ ) and 2 infection status levels (infected/uninfected *P. rubescens* cultures), for a total of 32 treatment combinations. We used 4 replicates at each combination, for a total of 128 experimental units. Fig. S1 shows a schematic illustrating the experimental design.

### Culture details and experimental conditions

*Planktothrix rubescens* strain NIVA-CYA98 and the chytrid parasite Chy-Kol2008 (Rhizophydiales) that were used in this study are monoclonal but non-axenic; bacterial biomass was kept low by semi-continuous growth, confirmed by microscopy. WC medium was used to grow *P. rubescens* [58], with silicon excluded as we were not experimenting with diatoms.

Before the start of the experiment the *P. rubescens* cultures were acclimatised to the different experimental conditions. Temperature was regulated by using heated water baths in a refrigerated room maintained at 4 °C, logged with calibrated temperature loggers (HOBO Onset, UX120-006M). Light was provided by fluorescent tubes (Osram neutral white, 4000 K), and light intensities were manipulated using neutral density filters to shade the culture flasks (manufactured by Lee Filters, Hampshire UK, filters numbers 211, 210, and 209). Light intensities were measured inside the shaded flasks (Licor LI-250A light meter, US-SQS/WB quantum sensor). Photoperiod was set to a 16:8 h light:dark cycle. The experiment was performed in 250 mL culture flasks (Greiner Bio One, Item No.: 658195). Cultures were shaken daily during acclimatisation and during the experiment.

At the start of the experiment, the culture flasks were filled with 100 mL of *P. rubescens* suspension, diluted to a biovolume of 4 nL  $\text{mL}^{-1}$ , so all treatments had the same density at the start of the experiment. Subsequently, half of these flasks were inoculated with a dense zoospore suspension, constituting the infected treatment. The zoospore suspension was made by filtering a heavily infected culture (16 °C, 11  $\mu\text{E m}^{-2} \text{s}^{-1}$ ) of *P. rubescens* through a glass serological pipette filled with loosely packed glass fibers that had been autoclaved. The glass fiber filter that is created this way lets through most of the zoospores but is highly efficient in removing the filaments of *P. rubescens*. One mL of this dense zoospore suspension was added to the infected treatment, resulting in 70 zoospores  $\text{mL}^{-1}$  at the start of the experiment. The experiment lasted for 20 days.

### Sampling and imaging

2 mL samples were taken every other day during the experiment and fixed in 0.5% final concentration glutaraldehyde. The samples were stored in 2 mL sample tubes at 4 °C.

To analyze the samples from 128 experimental units, a high throughput biovolume measurement method was developed (Wierenga et al., in prep). The method relies on high resolution composite images of the entire surface of a clear bottom well, imaged by an automated microscope. 300  $\mu\text{L}$  of each sample was pipetted in duplicate into a clear bottom 96-well plate (Greiner Bio one Item No: 655096) for image analysis. The plates were put in the fridge for 24 h, to allow enough time for settling of the filaments. Using a Biotek cytation-3, image composites were taken of the entire surface of each well bottom with a 4x magnification objective. Images were taken in the chlorophyll and phycoerythrin autofluorescence channel (586 nm excitation and 647 nm emission). This yields high quality images with bright filaments against a dark background, ideal for image analysis. For infection measurements 300  $\mu\text{L}$  fixed sample was pipetted in duplicate into clear-bottom 96-well plates. The plates were put in the fridge for 24 h, to allow enough time for settling of the filaments. To visualize the chytrid sporangia, 10  $\mu\text{L}$  calcofluor-white (CFW) was added to each well to get a 5  $\mu\text{g/mL}$  final solution. To increase fluorescence output of the CFW stain, 10  $\mu\text{L}$  of sodium hydroxide (pH > 13.5) was added to increase the pH in the well. After incubation for 10 min, the plates were imaged with the Biotek cytation-3, in three different channels: brightfield, chlorophyll and phycoerythrin autofluorescence (586 nm excitation, 647 nm emission), and CFW (377 nm excitation, 447 nm emission). These composite images were combined to generate images which clearly show the outline of the filaments and stained sporangia. Furthermore, the viability of filaments can be assessed from the autofluorescence signal in the images.

### Image analysis

To measure the biovolume, the autofluorescence image composites were analyzed with the open-source image analysis tool *ImageJ*, using the plugin *skeletonize*. In short, this method uses a ‘‘Skeletonization algorithm’’ to compute the total length of all filaments in a picture. These are subsequently converted to biovolume using the equation for calculating the volume of a cylinder ( $V = \pi r^2 l$ ), where  $r$  is the mean radius of filaments and  $l$  is the total length of all filaments. The method is robust and can

**Table 1.** Overview of all parameters and variables used in the dynamical model.

Symbol	Shape/Dependency	Meaning	Value/equation	Units
<b>Variables</b>				
$H_u$		Uninfected host		nL mL <sup>-1</sup>
$H_i$		Infected host		nL mL <sup>-1</sup>
$Z$		Free-swimming zoospores		cells mL <sup>-1</sup>
<b>Parameters</b>				
$K$	Constant	Carrying capacity	600	nL mL <sup>-1</sup>
$l$	GAM with temperature and light	Infectivity	GAM	mL cell <sup>-1</sup> day <sup>-1</sup>
$r$	GAM with temperature and light	Growth rate of the uninfected host	GAM	day <sup>-1</sup>
$m_u$	Exponential increase with temperature	Death rate of uninfected host	$m_u = 4.62 \cdot 10^{-4} \cdot e^{0.0783 \cdot T}$	day <sup>-1</sup>
$m_i$	Exponential increase with temperature	Death rate of infected host	$m_i = 0.0305 \cdot e^{0.117 \cdot T}$	day <sup>-1</sup>
$\rho$	Constant	Zoospore production per biovolume of infected host	20	cells nL <sup>-1</sup>
$m_z$	Exponential increase with temperature	Death rate of zoospores	$m_z = 0.035 \cdot e^{0.128 \cdot T}$	day <sup>-1</sup>
$\tau$	Exponential decrease with temperature	Development time of zoospores in sporangia	$\tau = 16.42 \cdot e^{-0.099 \cdot T}$	Time in days

Where possible parameters were based on data from our experiment or from previous experiments with closely related organisms. The dependence of the parameters on temperature, light or both is indicated.

handle relatively high concentrations in samples because overlapping of filaments is not a big problem. It requires only limited human input, reducing bias. Furthermore, with this method a relatively big sample of 300  $\mu$ L is measured in its entirety, compared to manual counting of only a fraction of that volume, thereby improving precision.

To measure infections during the experiment, a minimum of 50 filaments were measured in the composite infection images and marked as infected or uninfected. Instead of using the frequency of infected and uninfected filaments to calculate the prevalence of infection, we used the length of infected and uninfected filaments. This results in a better representation of the prevalence of infection because there is a large variation in length, and moreover, infected filaments are typically shorter than uninfected filaments (as also seen in [59]).

### Data analysis

Data analysis and graphing was done using R version 4.0.4 and RStudio [60, 61]. ggplot2 (version 3.3.5) was used to make the graphs and the data processing was done with the help of the tidyverse packages (version 1.3.1) [60–63]. Comparisons of means were done using the robust yuen t-test from the package PairedData version 1.1.1 [64].

### Dynamical model

We used a dynamical host – parasite model to assess the dependence of chytrid – phytoplankton dynamics on temperature and light. We modified a model from Frenken et al. 2020 [55] by making its parameters temperature- and light-dependent. The model consists of three equations, which track the dynamics of uninfected hosts ( $H_u$ ), infected hosts ( $H_i$ ) and free-swimming zoospores ( $Z$ ).

The uninfected host  $H_u$  follows logistic growth with a carrying capacity  $K$  (nL mL<sup>-1</sup>) and a growth rate  $r$  (day<sup>-1</sup>). Losses of uninfected host are defined by a density-independent mortality rate:  $m_u$  (day<sup>-1</sup>), and by infection of uninfected host by a zoospore, which converts uninfected host into infected host. The infectivity constant  $l$  (mL cell<sup>-1</sup>) is a measure for the infection efficiency of zoospores (mL cell<sup>-1</sup>).

$$\frac{dH_u}{dt} = rH_u \left(1 - \frac{H_u}{K}\right) - m_u H_u - lH_u Z \quad (1)$$

Infected hosts  $H_i$  increase with every uninfected host that gets infected by the attachment of a zoospore. This is the same element as the loss due to infection for the uninfected host ( $lH_u Z$ ). Infected host decreases with a density-independent mortality rate  $m_i$  (day<sup>-1</sup>) and with maturation of

sporangia given by the development time  $\tau$  (days). The maturation of sporangia assumes infected host  $H_i$  is converted into zoospores.

$$\frac{dH_i}{dt} = lH_u Z - \left(\frac{1}{\tau}\right) H_i - m_i H_i \quad (2)$$

Chytrid zoospores  $Z$  increase when sporangia develop with development time  $\tau$  and release new zoospores. The zoospore production parameter  $\rho$  (cells nL<sup>-1</sup>) defines the number of spores produced per biovolume of infected host. Spores are lost when they infect an uninfected host, and additionally at a density-independent mortality rate  $m_z$  (day<sup>-1</sup>).

$$\frac{dZ}{dt} = \left(\frac{\rho}{\tau}\right) H_i - lH_u Z - m_z Z \quad (3)$$

**Model parameter values.** Some model parameters (Table 1) were calculated directly from our experimental data: the infectivity parameter  $l$  and the growth rate  $r$ , making them functions of light and temperature. The infectivity parameter  $l$  is calculated by assuming exponential decay of  $H_u$  with  $Z$ , and is directly calculated from experimental data according to the following equation:

$$l = - \frac{\ln \left[ \frac{H_u(t)}{H_u(t_0)} \right]}{Z(t_0)t} \quad (4)$$

where  $t_0$  is the beginning of the experiment and  $t$  is the length of the chosen period over which  $l$  was calculated (2 days; see supplementary information for details). The phytoplankton growth rate  $r$  was determined by fitting an exponential model to *P. rubescens* density over time in the uninfected treatments. To run the dynamical model at a higher resolution for temperature and light than the intervals used for the experiment, a generalized additive model (GAM) was fitted to calculated values of  $r$  and  $l$  across the temperature and light levels used in the experiment. This GAM was subsequently used in the dynamical host – parasite model to generate values for  $r$  and  $l$  at interpolated temperature and light levels. The parameters  $K$  and  $\rho$  were kept constant. The carrying capacity was set at 600 (nL mL<sup>-1</sup>), based on a logistic fit to experimental data at high light and temperature. The production of zoospores  $\rho$  was calculated from supplementary data from Frenken et al. 2020 [55], which has zoospore production data on a very closely related strain of *P. rubescens* and chytrids. It is calculated by dividing newly produced zoospores by the biovolume of the host 2 days prior, and is found to be 20 cells nL<sup>-1</sup>, which was set for

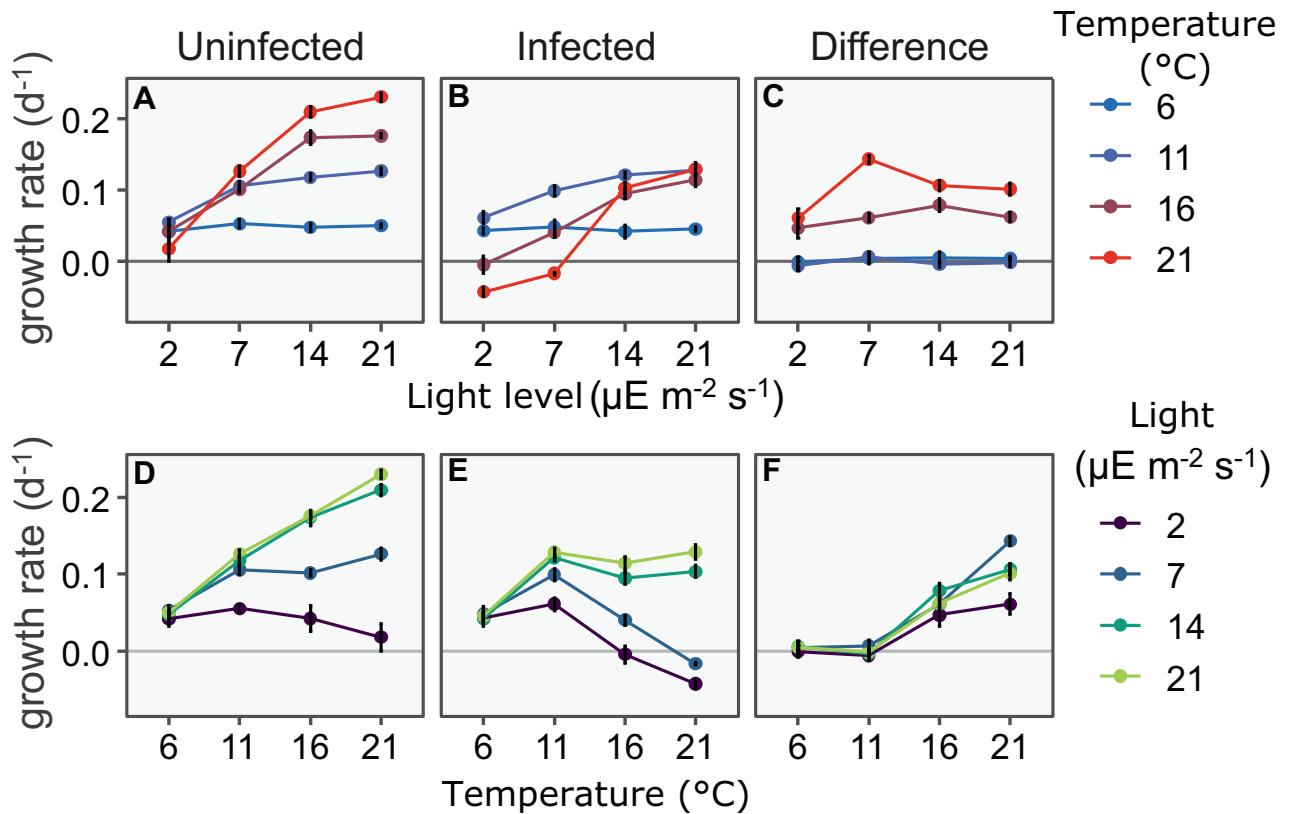


**Fig. 1** *Planktothrix* growth rate varies strongly with temperature, light and infection status. **A-C** Growth rate of uninfected and infected *P. rubescens* as a function of light at each of the 4 temperatures tested. The effect of the interaction between light and temperature is clearly visible both in infected and uninfected treatments. Infection reduces growth rate at 16 and 21 °C but not at 6 and 11 °C. Within each temperature, changing light has little effect on the difference in growth rate between infected and uninfected treatments. **D-F** The same data, viewed with temperature on X-axis and with light levels indicated by color. Within each light level, changing temperature has a large effect on the difference in growth rate between infected and uninfected treatments. In all panels dots represent mean growth rates and error bars represent the standard error of the mean.

each temperature and light combination. Infective lifetime of zoospores was found to be 2.71 days at 17 °C. This translates into a mortality rate  $m_z$  of 0.37 day<sup>-1</sup>, which we set to exponentially increase with temperature. Development time for sporangia is found to be between 2 and 3 days based on routine observations of infected cultures and is set to exponentially decrease with temperature. The dynamical model was analyzed in R using the R Package *deSolve*, version 1.28 [65].

There is no straightforward way to calculate the mortality rates  $m_u$  and  $m_i$  from available data; we therefore assumed  $m_u$  to be equal to 1% of the maximum growth rate at each temperature (i.e. growth rate at the highest light level, 21 µE.m<sup>-1</sup>.s<sup>-1</sup>). The mortality rate of infected *P. rubescens* is based on the same fit, with a 50 percent higher dependency on temperature and a higher initial value to account for the increased mortality due to infection. For more details about this temperature and light dependence, please refer to the supplementary information.

## RESULTS

### Temperature and light effects on uninfected and infected *Planktothrix* growth rates

Temperature and light interacted to shape the growth of *P. rubescens* and its susceptibility to chytrid infections (Fig. 1, Table 1). The expected cold refuge [10] occurred in our experiments at temperatures of 11 °C and lower; no infections occurred in this range. The growth rate of *P. rubescens* generally increased with both temperature and light at the levels tested in this experiment, but the shape of the interaction was complex. At low temperature, increasing light had little effect on growth. At low light, increasing temperature above 11 °C decreased growth rate (Fig. 1). Furthermore, the positive effect of temperature on the growth rate

increased with light, whereas the positive effect of light on the growth rate, increased only till 14 µE m<sup>-2</sup> s<sup>-1</sup> (Fig. 1D, lines on top of each other).

### Effects of chytrid infection on *Planktothrix* growth

Chytrids did not strongly affect the growth rate of *P. rubescens* at temperatures of 11 °C and lower. The growth rate remained essentially unchanged between the infected and uninfected treatment, confirming the refuge for *P. rubescens* at low temperatures (Fig. 1C). At temperatures of 16 °C and higher, the chytrid infection led to a substantially lower growth rate at all light levels tested. The reduction is similar across light levels (Fig. 1C). The biggest effect of the chytrid infection occurs at the highest temperature, with a big change in growth rate. This results in negative growth rates of *P. rubescens* at lower light levels (Fig. 1B, E). Growth of *P. rubescens* is very low at high temperature and low light (21 °C, 2 µE m<sup>-2</sup> s<sup>-1</sup>); infection led to further deterioration, resulting in negative growth rates for *P. rubescens* in the infected treatment (21 °C, at 2 and 7 µE m<sup>-2</sup> s<sup>-1</sup> and 16 °C at 2 µE m<sup>-2</sup> s<sup>-1</sup>).

### Temperature and light effects on chytrid growth and infection prevalence

Temperature and light interact to shape chytrid growth, as indicated by the varying prevalence of infection on the last day of the experiment (Fig. 2A), and the growth and development of the infected and uninfected fractions of the *Planktothrix* biovolume (Figs. 1, 2B). Temperature is a major factor for chytrid growth showing increased prevalence of infection, especially at high light

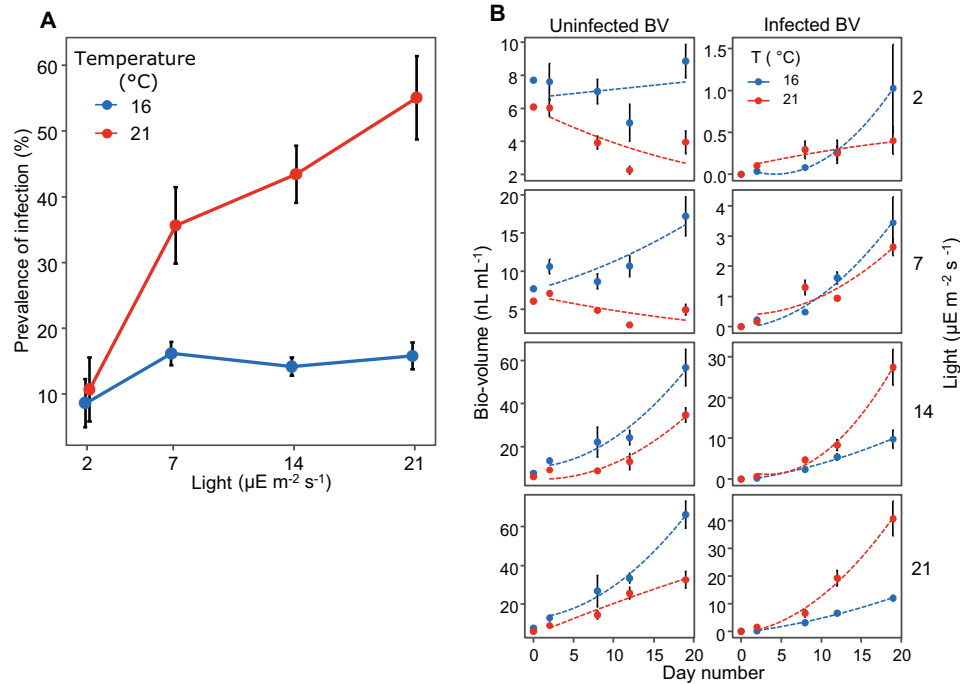


**Fig. 2** *P. rubescens* is affected more strongly by the chytrid parasite at 21 °C, especially at high light. **A** Prevalence of infection as a function of light level on the last day of the experiment. The prevalence of infection increases with increasing light at 21 °C, but not at 16 °C. At 6 and 11 °C no infected filaments were observed, and lines are not shown. **B** *P. rubescens* biovolume in the infected treatment, divided into uninfected and infected fractions; uninfected biovolume is shown in the left- and infected in the right-hand panels respectively.

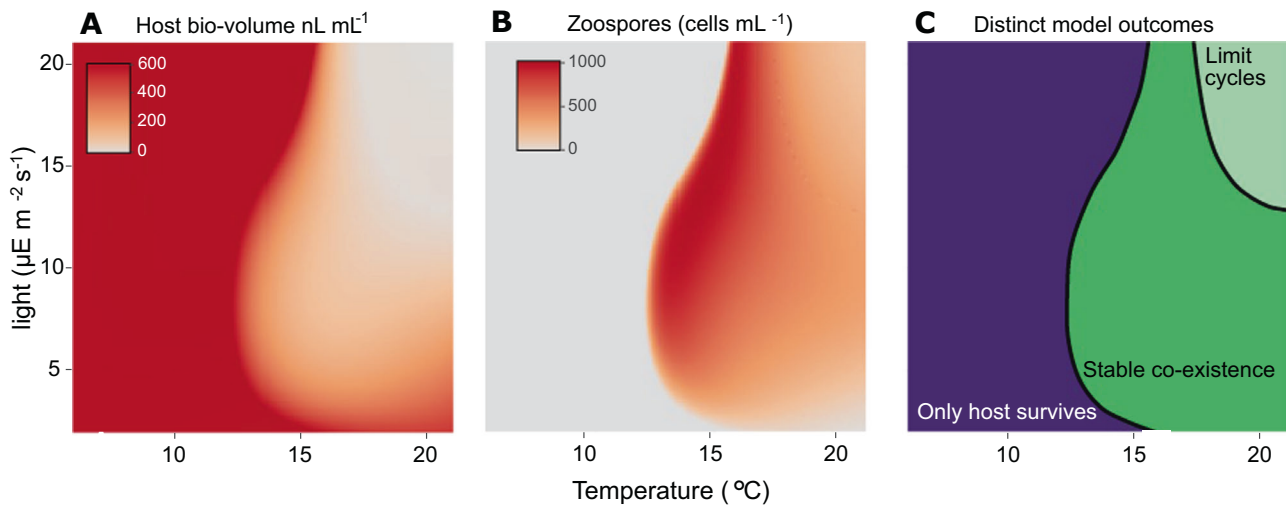


**Fig. 3** **Outcomes of modelled host-parasite dynamics in constant temperature and light conditions from our theoretical model.** Figure 4 shows example time series from individual points on the temperature-light surface. **A** Host biovolume is greatest at temperatures below 13 °C and decreases above it. At high temperatures, host biovolume decreases with increasing light. **B** Chytrid zoospore abundance is highest at intermediate temperature and medium-to-high light levels. **C** The model shows 3 possible outcomes. The host persists alone at low temperatures, it exhibits limit cycles at high temperature and high light, and it coexists stably at intermediate conditions. Abundances shown in the limit cycle region for panel **A** and **B** are averages over the course of one cycle. Note that the model is intended to explore qualitative outcomes across parameter space and not to make precise quantitative predictions, for which additional factors (such as nutrients) would need to be considered.

(Fig. 2A), and increased growth of infected BV with higher temperature (Fig. 2B). The effect of temperature is stronger at light. At the lowest light level ( $2 \mu\text{E m}^{-2} \text{s}^{-1}$ ), the effect of temperature is absent, and the prevalence of infection is similar between 16 °C and 21 °C. Chytrid growth, as indicated by the growing fraction of infected *P. rubescens* biovolume, was only higher at 21 °C than at 16 °C with light levels at or above  $14 \mu\text{E m}^{-2} \text{s}^{-1}$ . Furthermore,

growth of uninfected biovolume at 16 °C was higher than at 21 °C even though growth of *P. rubescens* in the uninfected treatment is higher at 21 °C than at 16 °C (Fig. 2B). This indicates that at 21 °C *P. rubescens* is more vulnerable to chytrid infection than at 16 °C, especially at higher light levels. At 21 °C increased light also leads to a greater increase of the prevalence of infection compared to 16 °C. We did not find a low light refuge for *P. rubescens*. On the contrary,

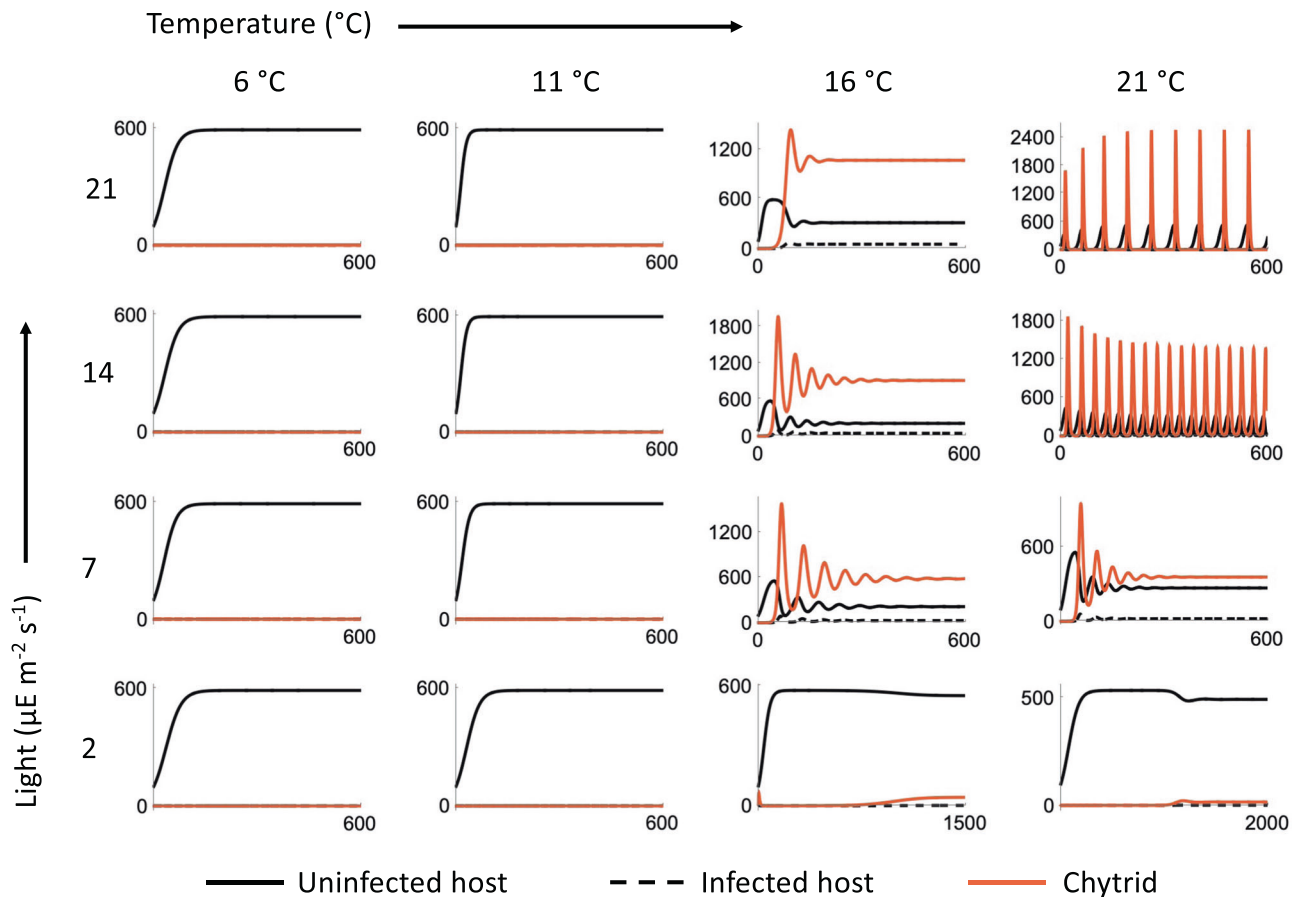


**Fig. 4 Example dynamics from the *P. rubescens* – chytrid model (summarized in Fig. 3), at the parameter combinations we measured experimentally.** The solid and dashed black lines indicate uninfected and infected host densities respectively, while the red line indicates the chytrid density. At low temperatures, *P. rubescens* has a thermal refuge and its density reaches the carrying capacity. With increasing light and temperature there is a shift from stable coexistence (16 °C with 7, 14, 21  $\mu\text{E m}^{-2} \text{s}^{-1}$ , and 21 °C with 7  $\mu\text{E m}^{-2} \text{s}^{-1}$ ) to limit cycles (21 °C with 14, 21  $\mu\text{E m}^{-2} \text{s}^{-1}$ ).

our experimental results show a large reduction in the growth rate of *P. rubescens* at low light with chytrid infection, especially at high temperatures (Fig. 1).

**Dynamical model.** We investigated how temperature and light would interact to drive *P. rubescens* - chytrid dynamics using a host – parasite model. We see a clear refugium defined largely by conditions of low temperature (Fig. 3), identified by high host density (Fig. 3A), the absence of zoospores (Fig. 3B) and the distinct outcomes of the model (the ‘only host’ region in Fig. 3C). The low temperature refuge is explained by the absence of chytrid infections at low temperature. This refuge is also dependent on light level; between approximately 13 and 15 °C, a refuge exists at very low light levels and at high (for this experiment) light levels, while intermediate light levels allow for persistence of the parasite. The highest densities of *P. rubescens* are found in refuge conditions and decrease with increasing temperature and light (Fig. 3A). The chytrid abundance is at its highest at an intermediate temperature between 14 and 16 °C, and light levels above 10  $\mu\text{E m}^{-2} \text{s}^{-1}$ .

Three distinct outcomes are observed at the different combinations of temperature and light we explored (Figs. 3C, 4). At low temperatures (<13 °C), only the uninfected host can survive irrespective of light levels (Fig. 3A). The host (uninfected and infected) and the chytrid coexist stably at intermediate to high temperatures (Fig. 3C). However, the temperature range for stable coexistence is drastically reduced at high light levels (Fig. 3C).

Finally, at high temperature and light levels, we find a limit cycle involving the uninfected host, infected host and the chytrid.

## DISCUSSION

### *P. rubescens* – chytrid growth and infection dynamics

We show that dynamics of *P. rubescens* and their chytrid parasites are heavily shaped by the interaction of temperature and light (Figs. 1–3). It has been previously shown that temperature and light are important factors in this host-parasite relationship [10, 11, 48, 49, 66, 67], but how this is affected by the interaction between temperature and light has not been well studied. To our knowledge, the only work on the interaction of temperature and light on chytrid-host dynamics is by Bruning [9], showing that in the diatom *Asterionella* and its chytrid parasite, that the two factors interact to affect infection dynamics. In *P. rubescens*, growth is most affected by chytrid infections at higher light and temperature levels. Even though we found relatively low infectivity of chytrids under low light, the intrinsic slow *Planktothrix* growth due to low light means that chytrids can still arrest *P. rubescens* growth in these conditions. We thus do not find a physiological refuge for *P. rubescens* at low light as we hypothesized and was found for *Asterionella* [9].

### Indirect light resource utilization by chytrids

The chytrids in this experiment are obligate parasites [68], feeding on the host as a resource, and thus light is not a direct resource for

the chytrids. Increased light does increase the release of dissolved organic carbon (DOC) by phytoplankton, affecting the affinity of zoospores to their host through chemotaxis and thus the interaction between the host and the parasite [9, 53, 69, 70]. However, here we find that at the lowest light level, increased temperature does not lead to increased prevalence of infection, and that increased light leads to a very small increase in the prevalence of infection at 16 °C. At 16 °C, temperature may be the limiting factor for chytrid growth, and more light does not lead to increased chytrid growth. At 21 °C however, the chytrid growth increases with light and thus might be resource-limited, with increased photosynthetic resources available at higher light intensity indicating indirect light utilization by acquiring energy resources from photosynthesis of the host while it is infected. Optimizing resource utilization by feeding while the host is actively photosynthesizing makes sense from an evolutionary perspective and is further suggested by the absence of a temperature effect at the lowest light level. This would not be expected if the chytrid uses only existing host resources at the time of infection for its reproduction and growth. Instead, it may feed off the host while alive, as occurs in most parasites [71]. A recent study has shown that increased light intensity and quality leads to bigger sporangia and increased chytrid transmission [11], indicating that chytrids indirectly utilize light through host photosynthesis. Another explanation could be that hosts grown under higher light stores more carbohydrates, and as such are a better energy source for the chytrid parasite.

### Dynamic model outcome and implications

The model shows three distinct outcomes over the range of conditions we explored: (1) only the host survives, (2) stable coexistence between the parasite and the host, and (3) limit cycles of host and parasite. (Figs. 3C, 4). Limit cycles occur at high temperatures and high light intensities (Figs. 3C, 4). Under these conditions, *P. rubescens* can grow rapidly but is vulnerable to infection, and infection under these conditions leads to a rapid decline of the host to very low densities. In nature, chytrids are found both at low densities with only minimal impact on the host [72–74], as well as at high densities and high infection incidence that can rapidly terminate host blooms [34, 44, 66, 75]. In natural conditions, it is possible that stochastic variation during periods of low density could lead to local extinction of both host and parasite, and so may not be congenial to the persistence of this host-parasite system despite the model outcome of limit cycles.

This suggests an interesting biotic alternative to abiotic factors explaining the niche of *P. rubescens*, which is almost always found around the 0.1–1% light level in stratified lakes [23]. The prevailing hypothesis is that they have adapted to a specific niche in the lake with relatively high nutrient levels, lower temperatures, and most importantly low light, where they outcompete other phytoplankton because they possess the accessory pigments phycoerythrin and phycocyanin [13]. However, this is not entirely consistent with the experimental data showing that growth rates of *P. rubescens* increase when temperature and light are increased beyond the limiting conditions found at the bottom of the euphotic zone; light levels up to 300  $\mu\text{E m}^{-2} \text{s}^{-1}$ , and temperatures up to at least 21 °C still promote growth [12, 13, 18, this study]. But at these high temperature and light levels, *P. rubescens* may be very sensitive to chytrid infections and therefore unable to sustain growth, especially in competition with other phytoplankton species. Chytrid infection might thus limit *P. rubescens* to regions of the water column that are suboptimal for its growth but safe from infection. If so, temperature, light and chytrids may together determine the vertical distribution of *P. rubescens* in stratified lakes. The model furthermore shows that the thermal refuge extends to higher temperatures at higher light levels, although we do not have experimental data to confirm this. We also cannot say whether a high-temperature refuge also exists as in the case of *P.*

*agardhii* and *A. formosa* [48, 49]. Our explanation here for the *P. rubescens* vertical distribution would only hold if there was no such high-temperature refuge.

Although we believe this model offers us useful insights into the *P. rubescens* vertical distribution, its purpose is not to make precise quantitative predictions but instead to explore how temperature-light interactions may affect host-parasite dynamics. To make reliable quantitative predictions, the model would likely need to account for several additional factors, including nutrient dynamics, temperature & light variation, and the effects of sinking, all of which we ignore here. Also, for some model parameter values, we used estimates based on the literature instead of measurements from our experiments (Table 1). These estimates are based on empirical data and physiological understanding, but there is unavoidable uncertainty about their true values. The values we chose may have led to lower prevalence of infection in the model (Fig. 3) than that seen in our experiments (Fig. 2), suggesting that some of these parameters could be improved upon if a predictive model is developed in future.

### CONCLUSION

We have shown that the host – parasite interaction of *P. rubescens* and chytrids is strongly affected by the interaction between temperature and light. Our results confirm the existence of a thermal refugium below at least 11 °C, and that this may vary with light intensity although there appears to be no specific low light refuge. In general, vulnerability of *P. rubescens* to chytrid infections increases with temperature and light. This may explain why *P. rubescens* is hardly ever found under warmer or high-light conditions in nature, even though lab experiments show that these conditions lead to higher growth rates in the absence of chytrids. Our model does neglect some important complexities, such as the effects of nutrients on the biotic interaction, and the effects of light on host stoichiometry and consequently chytrid growth. Our results highlight how abiotic and biotic environmental factors can interact in complex ways to affect ecological dynamics.

### DATA AVAILABILITY

The datasets generated and analysed during the current study are freely available at <https://doi.org/10.5281/zenodo.7014420>.

### REFERENCES

1. Díez B, Ininbergs K. Ecological importance of cyanobacteria. In *Cyanobacteria* (pp. 41–63). John Wiley & Sons, Ltd. (2013) <https://doi.org/10.1002/9781118402238.ch3>
2. Fristachi A, Sinclair JL, Hall S, Berkman JAH, Boyer G, Burkholder J, et al. Occurrence of cyanobacterial harmful algal blooms workgroup report. *Adv Experimental Med Biol.* 2008;619:45–103. [https://doi.org/10.1007/978-0-387-75865-7\\_3](https://doi.org/10.1007/978-0-387-75865-7_3)
3. Huisman J, Codd GA, Paerl HW, Ibelings BW, Verspagen JMH, Visser PM. Cyanobacterial blooms. *Nat Rev Microbiol.* 2018;16:471–83. <https://doi.org/10.1038/s41579-018-0040-1>
4. Plaas HE, Paerl HW. Toxic Cyanobacteria: A Growing Threat to Water and Air Quality. In *Environmental Science and Technology* (Vol. 55, Issue 1, pp. 44–64). American Chem Soc. 2021. <https://doi.org/10.1021/acs.est.0c06653>
5. Kurmayer R, Deng L, Entfellner E. Role of toxic and bioactive secondary metabolites in colonization and bloom formation by filamentous cyanobacteria Planktothrix. *Harmful Algae.* 2016;54:69–86. <https://doi.org/10.1016/j.hal.2016.01.004>
6. Rohrlack T, Christiansen G, Kurmayer R. Putative antiparasite defensive system involving ribosomal and nonribosomal oligopeptides in cyanobacteria of the genus planktothrix. *Appl Environ Microbiol.* 2013;79:2642–7. <https://doi.org/10.1128/AEM.03499-12>
7. Legnani E, Copetti D, Oggioni A, Tartari G, Palumbo MT, Morabito G. Planktothrix rubescens' seasonal dynamics and vertical distribution. *J Limnol.* 2005;64:61–73.
8. Walsby A, Ng G, Dunn C, Davis PA. Comparison of the depth where Planktothrix rubescens stratifies and the depth where the daily insolation supports its neutral

- buoyancy. *New Phytologist*. 2004;162:133–45. <https://doi.org/10.1111/j.1469-8137.2004.01020.x>
9. Bruning K. Effects of temperature and light on the population dynamics of the *Asterionella*-*Rhizophyidium* association. *J Plankton Res*. 1991a;13:707–19. <https://doi.org/10.1093/plankt/13.4.707>
  10. Rohrlack T, Haande S, Molversmyr Å, Kyle M. *Environmental Conditions Determine the Course and Outcome of Phytoplankton Chytridiomycosis*. 2015;1–17. <https://doi.org/10.1371/journal.pone.0145559>
  11. Tao Y, Wolinska J, Hölker F, Agha R. Light intensity and spectral distribution affect chytrid infection of cyanobacteria via modulation of host fitness. *Parasitology*. 2020;147:1206–15. <https://doi.org/10.1017/S0031182020000931>
  12. Davis PA, Walsby A. Comparison of measured growth rates with those calculated from rates of photosynthesis in *Planktothrix* spp. isolated from Blelham Tarn, English Lake District. *New Phytologist*. 2002;156:225–39. <https://doi.org/10.1046/j.1469-8137.2002.00495.x>
  13. Oberhaus L, Briand JF, Leboulanger C, Jacquet S, Humbert JF. Comparative effects of the quality and quantity of light and temperature on the growth of *Planktothrix agardhii* and *P. rubescens* 1. *J Phycol*. 2007;43:1191–9. <https://doi.org/10.1111/j.1529-8817.2007.00414.x>
  14. Reynolds CS Growth and replication of phytoplankton. In *The Ecology of Phytoplankton* (pp. 145–77). Cambridge University Press (2009). <https://doi.org/10.1017/CBO9780511542145.005>
  15. Litchman E, Klausmeier CA. Trait-based community ecology of phytoplankton. *Ann Rev Ecol, Evol, Syst*. 2008;39:615–39.
  16. Edwards KF, Thomas MK, Klausmeier CA, Litchman E. Phytoplankton growth and the interaction of light and temperature: A synthesis at the species and community level. *Limnol Oceanography*. 2016;61:1232–44.
  17. Thomas MK, Kremer CT, Litchman E. Environment and evolutionary history determine the global biogeography of phytoplankton temperature traits. *Global Ecol Biogeog*. 2016;25:75–86. <https://doi.org/10.1111/geb.12387>
  18. Bright DJ, Walsby A. The daily integral of growth by *Planktothrix rubescens* calculated from growth rate in culture and irradiance in Lake Zürich. *New Phytologist*. 2000;146:301–16. <https://doi.org/10.1046/j.1469-8137.2000.00640.x>
  19. Jann-Para G, Schwob I, Feuillade M. Occurrence of toxic *Planktothrix rubescens* blooms in lake Nantua, France. *Toxicol*. 2004;43:279–85.
  20. Jacquet S, Briand JF, Leboulanger C, Avois-Jacquet C, Oberhaus L, Tassin B, et al. The proliferation of the toxic cyanobacterium *Planktothrix rubescens* following restoration of the largest natural French lake (Lac du Bourget). *Harmful Algae*. 2005;4:651–72.
  21. Lenard T. Metalimnetic bloom of *Planktothrix rubescens* in relation to environmental conditions. *Oceanological Hydrobiological Studies*. 2009;38:45–53.
  22. Van den Wyngaert S, Salcher MM, Pernthaler J, Zeder M, Posch T. Quantitative dominance of seasonally persistent filamentous cyanobacteria (*Planktothrix rubescens*) in the microbial assemblages of a temperate lake. *Limnol Oceanogr*. 2011;56:97–109.
  23. Walsby A. Stratification by cyanobacteria in lakes: A dynamic buoyancy model indicates size limitations met by *Planktothrix rubescens* filaments. *New Phytologist*. 2005;168:365–76. <https://doi.org/10.1111/j.1469-8137.2005.01508.x>
  24. Conroy JD, Kane DD, Quinlan EL, Edwards WJ, Culver DA. Abiotic and biotic controls of phytoplankton biomass dynamics in a freshwater tributary, estuary, and large lake ecosystem: Sandusky bay (lake erie) chemostat. *Inland Waters*. 2017;7:473–92. <https://doi.org/10.1080/20442041.2017.1395142>
  25. Sommer U, Maciej Gliwicz Z, Lampert W, Duncan A. The PEG-model of seasonal succession of planktonic events in fresh waters. *Archiv Für Hydrobiologie*. 1986;106:433–71.
  26. Sommer U, Adrian R, De Senerpont Domis L, Elser JJ, Gaedke U, Ibelings B, et al. Beyond the plankton ecology group (PEG) model: Mechanisms driving plankton succession. *Ann Rev Ecol, Evol, Syst*. 2012;43:429–48. <https://doi.org/10.1146/annurev-ecolsys-110411-160251>
  27. Hatcher MJ, Dunn AM *Parasites in ecological communities: from interactions to ecosystems*. Cambridge University Press (2011).
  28. Marcogliese DJ. Parasites: Small Players with Crucial Roles in the Ecological Theater. *EcoHealth*. 2004;1:151–64. <https://doi.org/10.1007/s10393-004-0028-3>
  29. Sime-Ngando T, Lafferty KD, Biron DG. Roles and Mechanisms of Parasitism in Aquatic Microbial Communities. 2007. <https://doi.org/10.3389/978-2-88919-588-6>
  30. Frenken T, Alacid E, Berger SA, Bourne EC, Gerphagnon M, Grossart HP, et al. Integrating chytrid fungal parasites into plankton ecology: research gaps and needs. *Environmental Microbiology*. 2017;19:3802–22. <https://doi.org/10.1111/1462-2920.13827>
  31. Brussaard CPD, Kuipers B, Veldhuis MJW. A mesocosm study of *Phaeocystis globosa* population dynamics: I. Regulatory role of viruses in bloom control. *Harmful Algae*. 2005;4:859–74. <https://doi.org/10.1016/j.hal.2004.12.015>
  32. Gerphagnon M, Macarthur DJ, Gachon C, Van Ogtrop F, Latour D, et al. *The biological factors affecting the dynamics of cyanobacterial blooms*. 2009.
  33. Gleason FH, Jephcott TG, Küpper FC, Gerphagnon M, Sime-Ngando T, Karpov SA, et al. Potential roles for recently discovered chytrid parasites in the dynamics of harmful algal blooms. *Fungal Biol Rev*. 2015;29:20–33. <https://doi.org/10.1016/j.fbr.2015.03.002>
  34. Ibelings BW, Gsell AS, Mooij WM, Van Donk E, Van Den Wyngaert S, De Senerpont Domis LN. Chytrid infections and diatom spring blooms: Paradoxical effects of climate warming on fungal epidemics in lakes. *Freshwater Biol*. 2011;56:754–66. <https://doi.org/10.1111/j.1365-2427.2010.02565.x>
  35. Kagami M, De Bruin A, Ibelings BW, Van Donk E. Parasitic chytrids: Their effects on phytoplankton communities and food-web dynamics. *Hydrobiologia*. 2007;578:113–29. <https://doi.org/10.1007/s10750-006-0438-z>
  36. Lips KR, Brem F, Brenes R, Reeve JD, Alford RA, Voyles J, et al. Emerging infectious disease and the loss of biodiversity in a Neotropical amphibian community. *PNAS*. 2005;103:3165–70.
  37. McKenzie VJ, Peterson AC. Pathogen pollution and the emergence of a deadly amphibian pathogen. *Molecular Ecol*. 2012;21:5151–4. <https://doi.org/10.1111/mec.12013>
  38. Skerratt LF, Berger L, Speare R, Cashins S, McDonald KR, Phillott AD, et al. Spread of chytridiomycosis has caused the rapid global decline and extinction of frogs. *EcoHealth*. 2007;4:125–34. <https://doi.org/10.1007/s10393-007-0093-5>
  39. Ibelings BW, De Bruin A, Kagami M, Rijkeboer M, Brehm M, Van Donk E. Host parasite interactions between freshwater phytoplankton and chytrid fungi (*Chytridiomycota*). *J Phycol*. 2004;40:437–53.
  40. Bosch J, Martínez-Solano I, García-París. Evidence of a chytrid fungus infection involved in the decline of the common midwife toad (*Alytes obstetricans*) in protected areas of central Spain. *Biological Conserv*. 2001;97:331–7. [https://doi.org/10.1016/S0006-3207\(00\)00132-4](https://doi.org/10.1016/S0006-3207(00)00132-4)
  41. Bruning K, Lingeman R, Ringelberg J. Estimating the impact of fungal parasites on phytoplankton populations. *Limnol Oceanogr*. 1992;37:252–60. <https://doi.org/10.4319/lo.1992.37.2.0252>
  42. Paterson RA. Infestation of Chytridiaceae Fungi on Phytoplankton in Relation to Certain Environmental Factors. *Ecology*. 1960;41:416–24. <https://doi.org/10.2307/1933316>
  43. Şen B. Fungal parasitism of planktonic algae in Shearwater. IV: Parasitic occurrence of a new chytrid species on the blue-green alga *Microcystis aeruginosa* Kuetz. emend. Elenkin. 1998.
  44. van Donk E, Ringelberg J. The effect of fungal parasitism on the succession of diatoms in Lake Maarsveen I. *Netherlands Freshwater Biol*. 1983;13:241–51. <https://doi.org/10.1111/j.1365-2427.1983.tb00674.x>
  45. Agha R, Saebelfeld M, Manthey C, Rohrlack T, Wolinska J. Chytrid parasitism facilitates trophic transfer between bloom-forming cyanobacteria and zooplankton (*Daphnia*). *Scientific Rep*. 2016;6. <https://doi.org/10.1038/srep35039>
  46. Frenken T, Wierenga J, van Donk E, Declerck SAJ, de Senerpont Domis LN, Rohrlack T, et al. Fungal parasites of a toxic inedible cyanobacterium provide food to zooplankton. *Limnol Oceanogr*. 2018;63:2384–93. <https://doi.org/10.1002/lno.10945>
  47. Kagami M, von Elert E, Ibelings BW, de Bruin A, van Donk E. The parasitic chytrid, *Zygorhizidium*, facilitates the growth of the cladoceran zooplankton, *Daphnia*, in cultures of the inedible alga, *Asterionella*. *Proc Biological Sci/ Royal Soc*. 2007;274:1561–6. <https://doi.org/10.1098/rspb.2007.0425>
  48. Gsell AS, de Senerpont Domis LN, van Donk E, Ibelings BW. Temperature alters host genotype-specific susceptibility to chytrid infection. *PLoS One*. 2013;8:e71737. <https://doi.org/10.1371/journal.pone.0071737>
  49. McKindles KM, Manes MA, McKay RM, Davis TW, Bullerjahn GS. Environmental factors affecting chytrid (*Chytridiomycota*) infection rates on *Planktothrix agardhii*. *J Plankton Res*. 2021a;43:658–72.
  50. Fallowfield HJ, Daft MJ. The extracellular release of dissolved organic carbon by freshwater cyanobacteria and algae and the interaction with *Lysobacter* CP-1. *Br Phycol J*. 1988;1617:317–26. <https://doi.org/10.1080/00071618800650351>
  51. Mueller B, den Haan J, Visser PM, Vermeij MJA, van Duyl FC. Effect of light and nutrient availability on the release of dissolved organic carbon (DOC) by Caribbean turf algae. *Scientific Rep*. 2016;6:1–9. <https://doi.org/10.1038/srep23248>
  52. Bruning K. Infection of the diatom *Asterionella* by a chytrid. II. Effects of light on survival and epidemic development of the parasite. *J Plankton Res*. 1991c;13:119–29. <https://doi.org/10.1093/plankt/13.1.119>
  53. Van den Wyngaert S, Gsell AS, Spaak P, Ibelings BW. Herbicides in the environment alter infection dynamics in a microbial host-parasite system. *Environ Microbiol*. 2013;15:837–47. <https://doi.org/10.1111/j.1462-2920.2012.02874.x>
  54. Almcocera AES, Hsu SB, Sy PW. Extinction and uniform persistence in a microbial food web with mycoloop: Limiting behavior of a population model with parasitic fungi. *Mathematical Biosci Eng*. 2019;16:516–37.
  55. Frenken T, Miki T, Kagami M, Van de Waal DB, Van Donk E, Rohrlack T, et al. The potential of zooplankton in constraining chytrid epidemics in phytoplankton hosts. *Ecology*. 2020;101. <https://doi.org/10.1002/ecy.2900>



56. Gerla DJ, Gsell AS, Kooi BW, Ibelings BW, Van Donk E, Mooij WM. Alternative states and population crashes in a resource-susceptible-infected model for planktonic parasites and hosts. *FMeier, M. H. et al. (2015) Neuropsychological Decline in Schizophrenia from the Premorbid to Post-Onset Period: Evidence from a Population-Representative Longitudinal Study. American J Psychiatry.* 2013;58:538–51. <https://doi.org/10.1111/fwb.12010>
57. Miki T, Takimoto G, Kagami M. Roles of parasitic fungi in aquatic food webs: A theoretical approach. *Freshwater Biol.* 2011;56:1173–83. <https://doi.org/10.1111/j.1365-2427.2010.02562.x>
58. Guillard RRL, Lorenzen CJ. Yellow-green algae with chlorophyllid C. In *Phycology.* 1972;8:10–14.
59. McKindles KM, Jorge AN, McKay RM, Davis TW, Bullerjahn GS. Isolation and characterization of Rhizophydiales (Chytridiomycota), obligate parasites of *Planktothrix agardhii* in a Laurentian Great Lakes embayment. *Appl Environ Microbiol.* 2021b;87:e02308–20.
60. R Core Team. (2021). *R: A Language and Environment for Statistical Computing.*
61. RStudio Team. (2021). *RStudio: Integrated Development Environment for R* (1.4.1106).
62. Wickham, H (2016). *ggplot2: Elegant Graphics for Data Analysis.* Springer-Verlag New York.
63. Wickham H, Averick M, Bryan J, Chang W, McGowan LD, François R, et al. Welcome to the [tidyverse]. *J Open Source Software.* 2019;4:1686. <https://doi.org/10.21105/joss.01686>
64. Champely, S (2018). *PairedData* (1.1.1).
65. Soetaert K, Petzoldt T, Setzer RW. Solving Differential Equations in {R}: Package deSolve. *J Statistical Software.* 2010;33:1–25. <https://doi.org/10.18637/jss.v033.i09>
66. Frenken T, Velthuis M, de Senerpont Domis LN, Stephan S, Aben R, Kosten S, et al. Warming accelerates termination of a phytoplankton spring bloom by fungal parasites. *Global Change Biol.* 2016;22:299–309. <https://doi.org/10.1111/gcb.13095>
67. Scholz B, Vyverman W, Küpper FC, Ólafsson HG, Karsten U. Effects of environmental parameters on chytrid infection prevalence of four marine diatoms: A laboratory case study. *Botanica Marina.* 2017;60:419–31. <https://doi.org/10.1515/bot-2016-0105>
68. Sønstebo JH, Rohrlack T. Possible implications of Chytrid parasitism for population subdivision in freshwater cyanobacteria of the genus *Planktothrix*. *Appl Environ Microbiol.* 2011;77:1344–51. <https://doi.org/10.1128/AEM.02153-10>
69. Bruning K. Infection of the diatom *Asterionella* by a chytrid. I. Effects of light on reproduction and infectivity of the parasite. *J Plankton Res.* 1991b;13:103–17. <https://doi.org/10.1093/plankt/13.1.103>
70. Muehlstein LK, Amon JP, Leffler DL. Chemotaxis in the Marine Fungus *Rhizophyidium littoreum*. *Appl Environ Microbiol.* 1988;54:1668–72. <https://doi.org/10.1128/aem.54.7.1668-1672.1988>
71. Esch GW, Fernández JC. Introduction. In *A Functional Biology of Parasitism* (pp. 1–25). Springer Netherlands (1993). [https://doi.org/10.1007/978-94-011-2352-5\\_1](https://doi.org/10.1007/978-94-011-2352-5_1)
72. Gerphagnon M, Colombet J, Latour D, Sime-Ngando T. Spatial and temporal changes of parasitic chytrids of cyanobacteria. *Scientific Rep.* 2017;7:6056. <https://doi.org/10.1038/s41598-017-06273-1>
73. Maier MA, Peterson TD. Prevalence of chytrid parasitism among diatom populations in the lower Columbia River (2009–2013). *Freshwater Biol.* 2017;62:414–28. <https://doi.org/10.1111/fwb.12876>
74. Sime-Ngando T. Phytoplankton chytridiomycosis: Fungal parasites of phytoplankton and their imprints on the food web dynamics. *Front Microbiol.* 2012;3:361. <https://doi.org/10.3389/fmicb.2012.00361>
75. Kagami M, Urabe J. Mortality of the planktonic desmid, *Staurastrum dorsidentiferum*, due to interplay of fungal parasitism and low light conditions. *SIL Proceed.* 2002;28:1001–5. <https://doi.org/10.1080/03680770.2001.11901868>

## ACKNOWLEDGEMENTS

The authors gratefully acknowledge Thomas Rohrlack for early discussions which greatly helped putting us in the research direction described here, and Thijs Frenken & Takeshi Miki for discussions of their dynamic model and calculation of model parameters. This project was funded by the Swiss National Science Foundation (grant 31003A\_166260).

## AUTHOR CONTRIBUTIONS

BWI and JW designed the experiment. JW carried out the experiment. JW analysed and visualised the data with input from MKT and BWI. JW and RR analysed the theoretical model with input from MKT. JW, BWI & MKT wrote the paper, with input from RR.

## COMPETING INTERESTS

The authors declare no competing interests.

## ADDITIONAL INFORMATION

**Supplementary information** The online version contains supplementary material available at <https://doi.org/10.1038/s43705-022-00178-5>.

**Correspondence** and requests for materials should be addressed to Mridul K. Thomas.

**Reprints and permission information** is available at <http://www.nature.com/reprints>

**Publisher's note** Springer Nature remains neutral with regard to jurisdictional claims in published maps and institutional affiliations.



**Open Access** This article is licensed under a Creative Commons Attribution 4.0 International License, which permits use, sharing, adaptation, distribution and reproduction in any medium or format, as long as you give appropriate credit to the original author(s) and the source, provide a link to the Creative Commons license, and indicate if changes were made. The images or other third party material in this article are included in the article's Creative Commons license, unless indicated otherwise in a credit line to the material. If material is not included in the article's Creative Commons license and your intended use is not permitted by statutory regulation or exceeds the permitted use, you will need to obtain permission directly from the copyright holder. To view a copy of this license, visit <http://creativecommons.org/licenses/by/4.0/>.

© The Author(s) 2022